Inorganic Chemistry
Article

Inorg. Chem. **2009**, *48*, 9535–9542 **9535**
DOI: 10.1021/ic901109e

Di- and Tri-Zinc Catalysts for the Low-Pressure Copolymerization of CO_2 and Cyclohexene Oxide

Michael R. Kember, Andrew J. P. White, and Charlotte K. Williams*

Department of Chemistry, Imperial College London, London, SW7 2AZ, United Kingdom

Received June 9, 2009

The syntheses and characterization of three new macrocyclic proligands, with variation of the para aryl ring substituent, are reported. Dizinc and trizinc acetate complexes are prepared using these ligands and are characterized using infrared and nuclear magnetic resonance spectroscopies, mass spectrometry, elemental analysis, and, for the three trizinc complexes, single-crystal X-ray diffraction. The X-ray crystallographic and spectroscopic data indicate bridging and terminal acetate coordination modes, both in the solid state and in solution, for the trizinc complexes. All of the complexes show good turnover numbers and frequencies, under 1 atm of pressure of carbon dioxide, for the copolymerization of CO_2 and cyclohexene oxide to produce poly(cyclohexene carbonate). The electronic nature of the ancillary ligands' substituents influences the catalytic activity of the complex, with the electron-donating substituent reducing the activity. The dizinc catalysts show markedly higher activities than the trizinc analogues, suggesting that the coordination environment within the macrocycle is crucial to controlling the catalytic activity.

Introduction

In the current global climate, with high oil prices, increasing concern over global warming, and depleting petroleum resources, the development of renewable carbon sources is of the utmost importance. Carbon dioxide is a particularly attractive alternative feedstock as it is inexpensive, highly naturally abundant, and the byproduct of many industrial processes, including combustion.[1] The activation and use of carbon dioxide is challenging because it is thermodynamically very stable; hence, it has found relatively few large-scale, commercial applications. However, it is well established that various metal complexes activate it, and this opens up possibilities for metal-based catalytic reactions.[1−5]

The metal-catalyzed copolymerization of carbon dioxide and epoxides, to produce aliphatic polycarbonates, was first discovered 40 years ago by Inoue et al.[6] This land mark discovery led to the development of other catalytic copolymerization systems and the synthesis of a range of aliphatic polycarbonates.[7−10] Much recent research has focused on the copolymerization of cyclohexene oxide (CHO) and CO_2 (Scheme 1),[8,11−15] yielding poly(cyclohexene carbonate), which has a high glass transition temperature and reasonable tensile strength, but which is also degradable.[16]

Subsequent to Inoue et al.'s initial discovery, more active and controlled catalysts have been developed (Figure 1). The earliest catalysts were all based upon heterogeneous systems. Among the first discrete homogeneous catalysts were zinc phenoxide complexes; however, problems with catalyst aggregation led to undesirably large polycarbonate polydispersity indices.[17,18] More recently, activities have

*To whom correspondence should be addressed. E-mail: c.k.williams@imperial.ac.uk.

(1) Arakawa, H.; Aresta, M.; Armor, J. N.; Barteau, M. A.; Beckman, E. J.; Bell, A. T.; Bercaw, J. E.; Creutz, C.; Dinjus, E.; Dixon, D. A.; Domen, K.; DuBois, D. L.; Eckert, J.; Fujita, E.; Gibson, D. H.; Goddard, W. A.; Goodman, D. W.; Keller, J.; Kubas, G. J.; Kung, H. H.; Lyons, J. E.; Manzer, L. E.; Marks, T. J.; Morokuma, K.; Nicholas, K. M.; Periana, R.; Que, L.; Rostrup-Nielson, J.; Sachtler, W. M. H.; Schmidt, L. D.; Sen, A.; Somorjai, G. A.; Stair, P. C.; Stults, B. R.; Tumas, W. *Chem. Rev.* **2001**, *101*, 953–996.
(2) Aresta, M.; Dibenedetto, A. *Dalton Trans.* **2007**, 2975–2992.
(3) Leitner, W. *Coord. Chem. Rev.* **1996**, *155*, 247–247.
(4) Musie, G.; Wei, M.; Subramaniam, B.; Busch, D. H. *Coord. Chem. Rev.* **2001**, *219*, 789–820.
(5) Palmer, D. A.; Vaneldik, R. *Chem. Rev.* **1983**, *83*, 651–731.
(6) Inoue, S.; Koinuma, H.; Tsuruta, T. *J. Polym. Sci., Part B: Polym. Lett.* **1969**, *7*, 287–292.
(7) Coates, G. W.; Moore, D. R. *Angew. Chem., Int. Ed.* **2004**, *43*, 6618–6639.
(8) Darensbourg, D. *J. Chem. Rev.* **2007**, *107*, 2388–2410.
(9) Sugimoto, H.; Inoue, S. *J. Polym. Sci., Pol. Chem.* **2004**, *42*, 5561–5573.
(10) Nozaki, K. *Pure Appl. Chem.* **2004**, *76*, 541–546.
(11) Moore, D. R.; Cheng, M.; Lobkovsky, E. B.; Coates, G. W. *Angew. Chem., Int. Ed.* **2002**, *41*, 2599–2602.
(12) Moore, D. R.; Cheng, M.; Lobkovsky, E. B.; Coates, G. W. *J. Am. Chem. Soc.* **2003**, *125*, 11911–11924.
(13) Mang, S.; Cooper, A. I.; Colclough, M. E.; Chauhan, N.; Holmes, A. B. *Macromolecules* **2000**, *33*, 303–308.
(14) Darensbourg, D. J.; Yarbrough, J. C. *J. Am. Chem. Soc.* **2002**, *124*, 6335–6342.
(15) Bok, T.; Yun, H.; Lee, B. Y. *Inorg. Chem.* **2006**, *45*, 4228–4237.
(16) Koning, C.; Wildeson, J.; Parton, R.; Plum, B.; Steeman, P.; Darensbourg, D. J. *Polymer* **2001**, *42*, 3995–4004.
(17) Darensbourg, D. J.; Holtcamp, M. W.; Struck, G. E.; Zimmer, M. S.; Niezgoda, S. A.; Rainey, P.; Robertson, J. B.; Draper, J. D.; Reibenspies, J. H. *J. Am. Chem. Soc.* **1999**, *121*, 107–116.
(18) Darensbourg, D. J.; Wildeson, J. R.; Yarbrough, J. C.; Reibenspies, J. H. *J. Am. Chem. Soc.* **2000**, *122*, 12487–12496.

Published on Web 08/27/2009

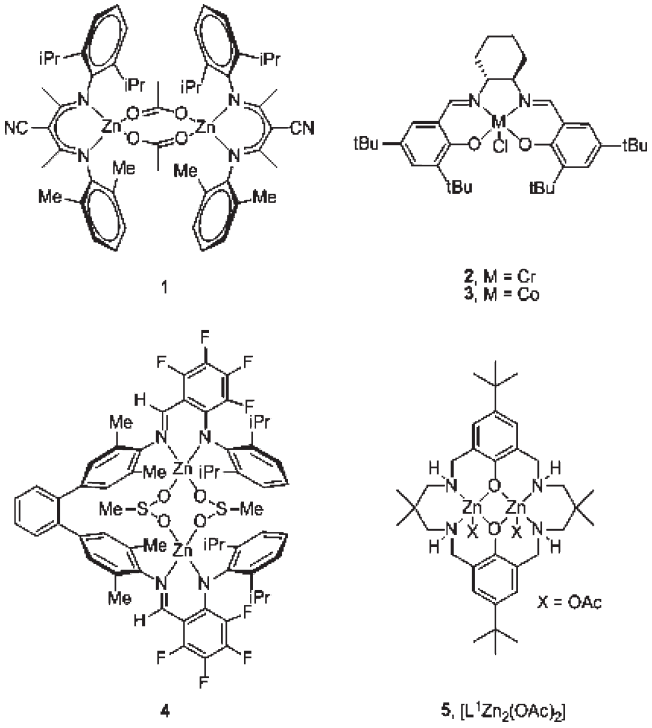

Figure 1. Active β-diiminate zinc (**1**), chromium/cobalt salen (**2**, **3**), anilido−aldimine zinc (**4**) catalysts, and $[L^1Zn_2(OAc)_2]$ (**5**).

Scheme 1. The Alternating Copolymerization of Carbon Dioxide and Cyclohexene Oxide, Forming Poly(cyclohexene carbonate), with Cyclic Cyclohexene Carbonate Produced As a Byproduct

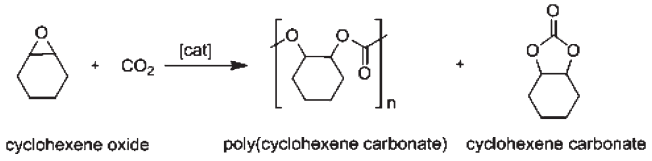

been significantly increased with the use of zinc β-diiminate (Figure 1; **1**)[12,19−22] and chromium(III) or cobalt(III) salen complexes (Figure 1; **2** and **3**).[8,14,23−27] A highly active (tetramethyltetraazaannulene)chromium(III) chloride catalyst has also been reported.[28] The zinc β-diiminate complexes, in particular, show very high turnover frequencies (TOFs), under relatively mild conditions. The most active of these complexes works under 7 atm of pressure at 50 °C,[11] compared to pressures of around 50−60 atm used for salen complexes.[8] In 2003, Coates et al. suggested that the most active β-diiminate complexes form loosely bound dimers under polymerization conditions.[12] Following on from this discovery, the preparation of various bimetallic complexes, particularly using zinc, has been reported.[15,29−32] Most notable among these are zinc anilido−aldimine (Figure 1; **4**) complexes which are active under extremely low catalyst loadings, thereby giving rise to high turnover numbers (TONs) and TOFs.[15,29]

There are, however, still significant limitations to the process, including low catalytic activities (TONs/TOFs) relative to conventional olefin polymerization catalysts, poor long-term catalyst stabilities, and the requirement for large CO_2 pressures (generally >7 atm). The development of catalysts active under milder conditions is favorable; latterly several catalysts active under only 1 atm CO_2 pressure have been reported.[12,31−34] Recently, we reported the most active of these catalysts, a bimetallic zinc acetate complex featuring a macrocyclic, reduced Robson-type[35−41] ligand, $[L^1Zn_2(OAc)_2]$ (Figure 1; **5**).[42] This catalyst is not only highly active under very low CO_2 pressures but it is also air-stable, robust, and capable of high TONs. It was also found to polymerize crude CHO with no loss in activity; this is in contrast to most other catalysts, which require rigorous purification of the CHO, by repeated distillations from drying agents.[43]

Previous catalyst structure−activity studies have established the profound influence that the ancillary ligands' electronic and steric properties have upon the TONs and TOFs.[7,8] In particular, electron-withdrawing groups, which are proposed to reduce the electron density on the metal center, have often led to higher TONs and TOFs.[11,15] The adaptation of H_2L^1, by substitution of the *para*-aryl substituent with various functional groups, was therefore investigated. Herein, we report the development of two new ligands, H_2L^2 and H_2L^3, and the preparation of bimetallic zinc acetate complexes. In addition, unusual trimetallic zinc acetate complexes of all three ligands are prepared, and the catalytic activities of all of the new complexes are compared.

Results and Discussion

Synthesis and Characterization. The preparation of the three macrocyclic proligands was carried out, using an

(19) Allen, S. D.; Moore, D. R.; Lobkovsky, E. B.; Coates, G. W. *J. Am. Chem. Soc.* **2002**, *124*, 14284–14285.
(20) Cheng, M.; Lobkovsky, E. B.; Coates, G. W. *J. Am. Chem. Soc.* **1998**, *120*, 11018–11019.
(21) Cheng, M.; Moore, D. R.; Reczek, J. J.; Chamberlain, B. M.; Lobkovsky, E. B.; Coates, G. W. *J. Am. Chem. Soc.* **2001**, *123*, 8738–8749.
(22) Eberhardt, R.; Allmendinger, M.; Luinstra, G. A.; Rieger, B. *Organometallics* **2003**, *22*, 211–214.
(23) Cohen, C. T.; Chu, T.; Coates, G. W. *J. Am. Chem. Soc.* **2005**, *127*, 10869–10878.
(24) Darensbourg, D. *J. Am. Chem. Soc.* **2005**, *127*, 14026–14038.
(25) Paddock, R. L.; Nguyen, S. T. *J. Am. Chem. Soc.* **2001**, *123*, 11498–11499.
(26) Qin, Z. Q.; Thomas, C. M.; Lee, S.; Coates, G. W. *Angew. Chem., Int. Ed.* **2003**, *42*, 5484–5487.
(27) Shi, L.; Lu, X. B.; Zhang, R.; Peng, X. J.; Zhang, C. Q.; Li, J. F.; Peng, X. M. *Macromolecules* **2006**, *39*, 5679–5685.
(28) Darensbourg, D. J.; Fitch, S. B. *Inorg. Chem.* **2007**, *46*, 5474–5476.
(29) Lee, B. Y.; Kwon, H. Y.; Lee, S. Y.; Na, S. J.; Han, S. I.; Yun, H. S.; Lee, H.; Park, Y. W. *J. Am. Chem. Soc.* **2005**, *127*, 3031–3037.
(30) Pilz, M. F.; Limberg, C.; Lazarov, B. B.; Hultzsch, K. C.; Ziemer, B. *Organometallics* **2007**, *26*, 3668–3676.
(31) Xiao, Y. L.; Wang, Z.; Ding, K. L. *Chem.—Eur. J.* **2005**, *11*, 3668–3678.
(32) Xiao, Y. L.; Wang, Z.; Ding, K. L. *Macromolecules* **2006**, *39*, 128–137.
(33) Sugimoto, H.; Kuroda, K. *Macromolecules* **2008**, *41*, 312–317.
(34) Sugimoto, H.; Ohshima, H.; Inoue, S. *J. Polym. Sci., Pol. Chem.* **2003**, *41*, 3549–3555.
(35) Pilkington, N. H.; Robson, R. *Aust. J. Chem.* **1970**, *23*, 2225–2236.
(36) Hoskins, B. F.; Robson, R.; Williams, G. A. *Inorg. Chim. Acta* **1976**, *16*, 121–133.
(37) Mandal, S. K.; Thompson, L. K.; Newlands, M. J.; Gabe, E. J.; Nag, K. *Inorg. Chem.* **1990**, *29*, 1324–1327.
(38) Mandal, S. K.; Thompson, L. K.; Newlands, M. J.; Gabe, E. J. *Inorg. Chem.* **1989**, *28*, 3707–3713.
(39) Atkins, A. J.; Black, D.; Blake, A. J.; MarinBecerra, A.; Parsons, S.; Ruiz-Ramirez, L.; Schroder, M. *Chem. Commun.* **1996**, 457–464.
(40) Okawa, H.; Furutachi, H.; Fenton, D. E. *Coord. Chem. Rev.* **1998**, *174*, 51–75.
(41) Atkins, A. J.; Black, D.; Finn, R. L.; Marin-Becerra, A.; Blake, A. J.; Ruiz-Ramirez, L.; Li, W. S.; Schroder, M. *Dalton Trans.* **2003**, 1730–1737.
(42) Kember, M. R.; Knight, P. D.; Reung, P. T. R.; Williams, C. K. *Angew. Chem., Int. Ed.* **2009**, *48*, 931–933.
(43) van Meerendonk, W. J.; Duchateau, R.; Koning, C. E.; Gruter, G. J. M. *Macromolecules* **2005**, *38*, 7306–7313.

Scheme 2. Two-Step Synthesis of the Macrocyclic Proligands from Various 2,6-Diformylphenols[a]

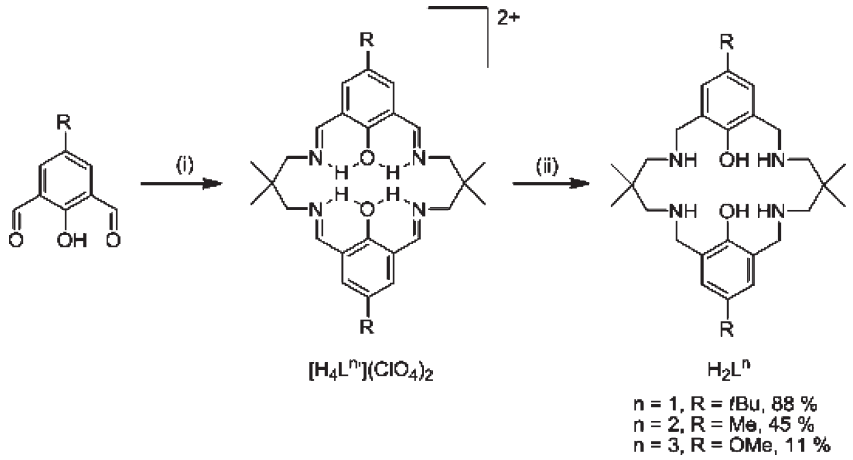

[a] (i) 2,2-dimethyl-1,3-propanediamine, AcOH, $NaClO_4$, MeOH, 25 °C, 20 h. (ii) $NaBH_4$, H_2O, MeOH, 25 °C.

Scheme 3. Synthesis of $[L^nZn_2(OAc)_2]$[a]

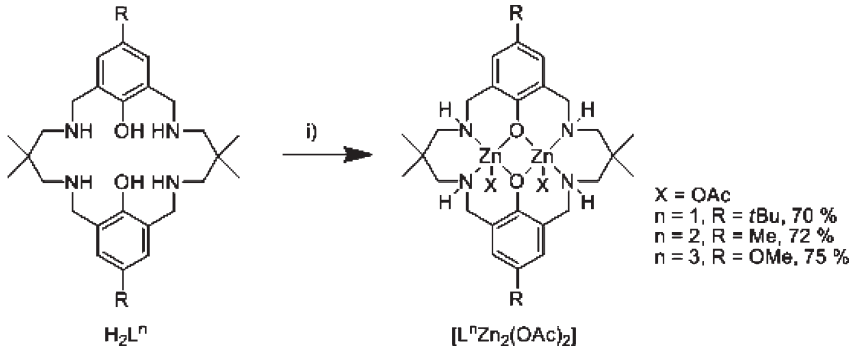

[a] (i) $2Zn(OAc)_2$, THF, 25 °C, 20 h.

adapted literature procedure, by reaction between the corresponding para-substituted 2,6-diformylphenols and 2,2-dimethyl-1,3-propanediamine (Scheme 2).[44,45] The synthesis involves the preparation and subsequent reduction of the macrocyclic imine perchlorate salts.[46] These salts are easily synthesized in high yields (76 − 95%) when R is a simple alkyl group ($[H_4L^{1,2'}](ClO_4)_2$); however, the introduction of groups that significantly alter the electronic nature of the aromatic ring promoted the formation of polymeric rather than macrocyclic products. This completely prevented the formation of macrocyclic perchlorate salts where R is an electron-withdrawing group, such as fluorine, and led to a reduced yield (35%) where R is an electron-donating methoxy group ($[H_4L^{3'}](ClO_4)_2$).

The reduction of the three perchlorate salts, $[H_4L^{n'}](ClO_4)_2$, proceeded easily using $NaBH_4$ in methanol; the corresponding reduced Robson-type proligands H_2L^1 and H_2L^2 were produced in good yields (88 and 59%, respectively). The reduction of $[H_4L^{3'}](ClO_4)_2$ was lower-yielding than those of the other two proligands (31%), possibly due to side reactions involving the methoxy group. ^1H and $^{13}C\{^1H\}$ NMR spectroscopies, electrospray ionization mass spectrometry, and elemental analyses confirmed the proligands' structures and purities.

Complexation reactions using the ligands, with 2 equiv of $Zn(OAc)_2$ in THF (Scheme 3), yielded the anticipated dizinc complexes $[L^nZn_2(OAc)_2]$. The syntheses all proceeded in good yields (∼ 70%, unoptimized), giving the complexes as white powders. The complexes' stoichiometries were confirmed by elemental analysis, the results of which are in excellent agreement with the theoretical values. The ^1H NMR spectra of the dizinc complexes are very broad, in all solvents at room temperature; this is attributed to the presence of various diastereoisomers, which are fluxional on the NMR time scale.[42] At 110 °C in d_2-tetrachloroethane (TCE), the peaks coalesce into a series of broadened resonances which can be assigned (Figure S11, Supporting Information). There are some common features to all of the NMR spectra, including a single resonance between 6.6 and 7 ppm, for the aromatic protons, and a broad resonance at approximately 4.7 ppm, corresponding to the four amine protons. The CH_2 groups are diastereotopic, producing four broadened resonances with integrals of 4H, as are the backbone CH_3 groups, which are split into two resonances, each with integrals of 6H, between 1 and 1.3 ppm. The alkyl resonances from the aromatic substituents are all observed with the expected chemical shifts and integrals. The fast-atom bombardment (FAB) mass spectra of all of the complexes show a fragment peak for the complexes less an acetate group.

(44) Lindoy, L. F.; Meehan, G. V.; Svenstrup, N. *Synthesis* **1998**, 1029–1032.
(45) Komatsu, N. *Org. Biomol. Chem.* **2003**, *1*, 204–209.
(46) Dutta, B.; Bag, P.; Adhikary, B.; Florke, U.; Nag, K. *J. Org. Chem.* **2004**, *69*, 5419–5427.

Scheme 4. Simplified Representation for the Synthesis of Novel Tri-Zinc Acetate Complexes, $[L^nZn_3(OAc)_4]$[a]

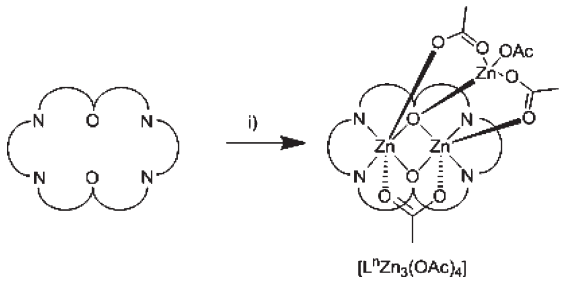

[a] (i) $4Zn(OAc)_2$, THF, 25 °C, 20 h. For complete structures, see the representations of the molecular structures from X-ray crystallography in Figures 2−4.

The reaction of H_2L^n with more than 2 equiv of $Zn(OAc)_2$ produced unusual trizinc tetra-acetate complexes, with molecular formula $[L^nZn_3(OAc)_4]$ (Scheme 4). While the ^1H NMR spectra of these complexes are similar to those of their bimetallic analogues in most solvents, the complexes are significantly less fluxional in CD_3OD: the spectra indicate the presence of one major and several minor isomers at room temperature (Figure S12, Supporting Information). This is particularly noticeable in the resonances corresponding to the aromatic and CH_3 protons, which have a series of lower-intensity resonances around the main peaks. As with $[L^nZn_2(OAc)_2]$, the CH_2 units are inequivalent; four multiplets each with an integral of approximately 4 are observed between 2.5 and 4.5 ppm. Upon heating to 50 °C, four sharp doublets are observed, as well as other low-intensity peaks corresponding to the minor isomers. No resonance is observed for the amine protons, which presumably exchange too rapidly with the solvent to be observed. The four acetate groups show a broad signal at 1.85 ppm, with an integral of 12. The $^{13}C\{^1H\}$ NMR spectra, at 110 °C in d_2-TCE (Figure S13, Supporting Information), are almost identical to those of $[L^nZn_2(OAc)_2]$, except for the presence of two methyl acetate resonances, at around 22 and 20 ppm, which indicate that the complexes contain different acetate binding modes.[47] This is confirmed by IR spectroscopy, where the presence of both bridging (C=O, 1588 and 1426 cm^{-1}) and terminal acetate (C=O, 1670 and 1369 cm^{-1}) coordination modes are observed.[48] The FAB mass spectra of the complexes show base peaks corresponding to the loss of a $Zn(OAc)_3$ moiety from the molecular ion. The trizinc complexes from all three ligands are easily crystallized; the crystals were analyzed using X-ray diffraction.

Complexes $[L^1Zn_3(OAc)_4]$, $[L^2Zn_3(OAc)_4]$, and $[L^3Zn_3(OAc)_4]$ crystallized with one, two, and three independent molecules in the asymmetric unit, respectively. Henceforth, these six complexes will be referred to as $[L^1Zn_3(OAc)_4]$, $[L^2Zn_3(OAc)_4]$-**I**, $[L^2Zn_3(OAc)_4]$-**II**, $[L^3Zn_3(OAc)_4]$-**I**, $[L^3Zn_3(OAc)_4]$-**II**, and $[L^3Zn_3(OAc)_4]$-**III**, and pictures for each can be found in Figures 2, 3, S4, 4, S7, and S9, respectively.

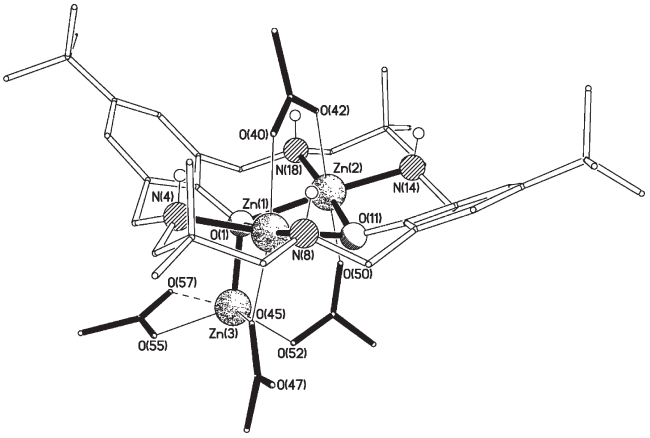

Figure 2. Molecular structure of $[L^1Zn_3(OAc)_4]$.

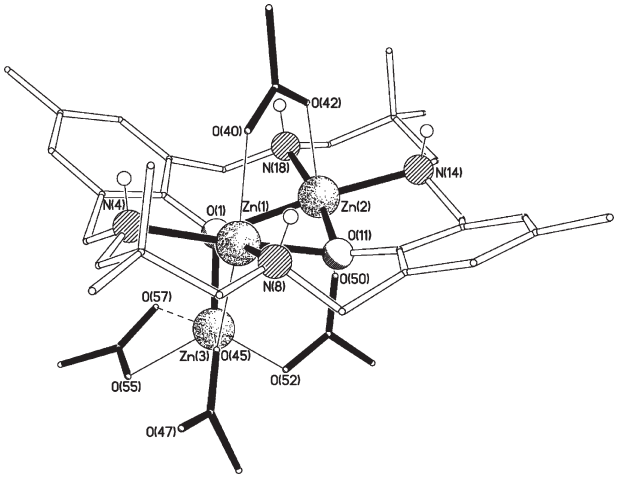

Figure 3. Molecular structure of one ($[L^2Zn_3(OAc)_4]$-**I**) of the two crystallographically independent complexes present in the crystals of $[L^2Zn_3(OAc)_4]$ (the other complex is shown in Figure S4, Supporting Information).

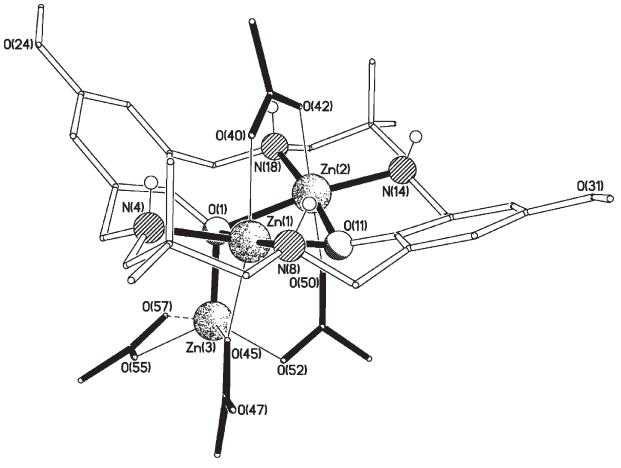

Figure 4. Molecular structure of one ($[L^3Zn_3(OAc)_4]$-**I**) of the three crystallographically independent complexes present in the crystals of $[L^3Zn_3(OAc)_4]$ (the other two complexes are shown in Figures S7 and S9, Supporting Information).

With the exception of the Zn(3) binding, the six complexes are very similar and have approximate mirror symmetry about a plane that passes through the Ar−O(1)

(47) Ye, B. H.; Wilhams, I. D.; Li, X. Y. *J. Inorg. Biochem.* **2002**, *92*, 128–136.

(48) Nakamoto, K. *Infrared and Raman Spectra of Inorganic and Coordination Compounds/Part B, Applications in Coordination, Organometallic, and Bioinorganic Chemistry*, 5th ed.; Wiley: New York, 1997.

Table 1. Comparative Bond Lengths (Å) for $[L^1Zn_3(OAc)_4]$, the Two Independent Molecules Present in the Crystals of $[L^2Zn_3(OAc)_4]$, and the Three Independent Molecules Present in the Crystals of $[L^3Zn_3(OAc)_4]$

	C(1)−O(1)	C(11)−O(11)	O(1)−Zn(1)	O(1)−Zn(2)	O(11)−Zn(1)	O(11)−Zn(2)
$[L^1Zn_3(OAc)_4]$	1.367(2)	1.348(2)	2.2843(14)	2.2027(14)	2.0587(14)	2.1003(13)
$[L^2Zn_3(OAc)_4]$-**I**	1.373(4)	1.351(4)	2.232(3)	2.215(3)	2.093(3)	2.054(3)
$[L^2Zn_3(OAc)_4]$-**II**	1.364(5)	1.347(4)	2.314(2)	2.253(2)	2.050(3)	2.068(2)
$[L^3Zn_3(OAc)_4]$-**I**	1.369(4)	1.351(5)	2.284(2)	2.245(3)	2.066(3)	2.092(3)
$[L^3Zn_3(OAc)_4]$-**II**	1.370(4)	1.360(4)	2.267(3)	2.183(3)	2.057(3)	2.087(3)
$[L^3Zn_3(OAc)_4]$-**III**	1.375(4)	1.357(5)	2.284(3)	2.228(3)	2.066(3)	2.102(3)

Table 2. Copolymerizations of CHO and CO_2 catalyzed using $[L^{1\text{-}3}Zn_2(OAc)_2]$ and $[L^{1\text{-}3}Zn_3(OAc)_4]$. Copolymerization conditions: 80 °C, 1 atm CO_2, 24 h

catalyst	TON[a]	TOF (h^{-1})[b]	% carbonate[c]	% copolymer[c]	M_n[d]	M_w/M_n[d]	% conversion[e]
$[L^1Zn_2(OAc)_2]$	220	9.2	>99	96	6200	1.19	45
$[L^2Zn_2(OAc)_2]$	199	8.3	>99	96	5800	1.21	40
$[L^3Zn_2(OAc)_2]$	144	6	>99	96	2800	1.21	29
$[L^1Zn_3(OAc)_4]$	96	4	>99	97	3400	1.21	29
$[L^2Zn_3(OAc)_4]$	73	3	>99	89	2800	1.22	22
$[L^3Zn_3(OAc)_4]$	47.9	1.9	>99	95	1400	1.21	14

[a] TON = number of moles of CHO consumed per mole of zinc. N/B: the copolymerization data for $[L^1Zn_2(OAc)_2]$ were previously reported with TON = number of moles of CHO consumed per mole of catalyst.[42] [b] TOF = TON per hour. [c] Determined by comparison of the integrals of signals arising from the methylene protons in the ^1H NMR spectra due to copolymer carbonate linkages (δ = 4.65 ppm), copolymer ether linkages (δ = 3.45 ppm), and the signals due to cyclic carbonate byproduct (δ = 4.0 ppm).[42] [d] Determined by SEC, in THF, using narrow polystyrene standards as calibrants. [e] Calculated by comparing the mass of polymer isolated against that expected at 100% conversion.

and Ar−O(11) bonds. The macrocyclic ligands all have dished conformations with all four N−H units on the same side of the ring. The octahedrally coordinated Zn(1) and Zn(2) atoms, which are bound within the ring, share the two ArO oxygen atoms O(1) and O(11) and are also bound to two proximal amine nitrogen atoms in each case. An acetate group bridges between these two metal centers in a bidentate fashion on the concave face of the dish. The bonding of the tetrahedrally coordinated Zn(3) moiety to this LZn_2 unit is essentially the same for five of the complexes, differing only for $[L^2Zn_3(OAc)_4]$-**II**. In this latter complex, the O(45)/O(47) and O(50)/O(52) acetate ligands both bind in bidentate bridging fashions, retaining the mirror symmetry, while in the other five complexes, the O(45)/O(47) acetate ligand adopts a monodentate bridging mode. (The dual bidentate bridging mode is also seen in the minor occupancy orientation of the disorder present in complex $[L^2Zn_3(OAc)_4]$-**I**, but this is only ca. 14% occupancy.)

The binding of the O(55)/O(57) acetate group varies in a more subtle manner across the six complexes. While the bond lengths to the bound oxygen O(55) fall within a narrow range [1.913(6)−2.034(3) Å], those to the nonbonded atom O(57) vary markedly between 2.361(4) and 3.025(4) Å (excluding the minor occupancy orientation of $[L^2Zn_3(OAc)_4]$-**I** where O(57) is actually bound to Zn(3) at 1.938(7) Å). Considering the Ar−O and ArO−Zn bond lengths (Table 1), two patterns emerge. In every complex, the Zn−O(1) bonds are longer than their Zn−O(11) counterparts, and related to this, in each complex, the Ar−O(1) bonds are longer than the Ar−O(11) bonds (but only in the case of $[L^1Zn_3(OAc)_4]$ is the difference statistically significant). Both of these observations can readily be explained by the presence of three zinc centers bonded to O(1), compared to the two zinc atoms bound to O(11). Unfortunately, in neither case can any pattern be discerned between the complexes; that is, the change in the para substituent has no noticeable effect on the structures.

Copolymerizations of CHO and CO_2. All of the new complexes were tested as catalysts for the copolymerization of cyclohexene oxide (CHO) and CO_2 (Table 2). All were excellent catalysts, active under very low pressures of CO_2 (just 1 atm). It should also be noted that all of the complexes are air-stable and robust, in contrast to previously reported zinc-based catalyst systems used for this reaction.

The bimetallic complexes, $[L^{1-3}Zn_2(OAc)_2]$, were tested at 1 atm of CO_2 and 80 °C. This temperature was chosen because it represents a compromise between activity, the desire to use the mildest conditions possible, and minimal production of cyclic carbonate.[42] While higher activities are achieved at 100 °C, over 5% cyclic carbonate was produced at this temperature using $[L^1Zn_2(OAc)_2]$.[42] $[L^1Zn_2(OAc)_2]$ was the most active catalyst of the series, with a TOF of 9 h^{-1}, 3 times higher than the best literature catalyst at this low pressure.[31] A clear relationship between the ligand structure and activity can be seen; as expected, $[L^3Zn_2(OAc)_2]$ is less active than $[L^{1or2}Zn_2(OAc)_2]$, giving a TOF of 6 h^{-1}. It should be noted that even this slight reduction in TOF still results in catalysts that are twice as active as the leading literature catalysts, at this pressure. It is proposed that the reduction in activity, using the electron-donating methoxy substituent, results from a decrease in zinc Lewis acidity and a concomitant decrease in binding and activation of CHO and CO_2. Alkyl substituents do not exert any significant electronic influence on the Lewis acidity of the zinc centers and as a result are more active. There is little difference in the activities of $[L^1Zn_2(OAc)_2]$ and $[L^2Zn_2(OAc)_2]$, the latter being slightly less active. As the substitution is quite far from the active site, it is expected that any steric effect is minimal. Instead, it is likely that this slight difference relates to the improved solubility of $[L^1Zn_2(OAc)_2]$ in CHO.

The ^1H NMR spectra of the copolymers show no evidence of ether linkages, produced by the homopolymerization of CHO. The absence of ether linkages is

Table 3. Crystallographic Data for Compounds $[L^1Zn_3(OAc)_4]$, $[L^2Zn_3(OAc)_4]$, and $[L^3Zn_3(OAc)_4]$

data	$[L^1Zn_3(OAc)_4]$	$[L^2Zn_3(OAc)_4]$	$[L^3Zn_3(OAc)_4]$
chemical formula	$C_{42}H_{66}N_4O_{10}Zn_3$	$C_{36}H_{54}N_4O_{10}Zn_3$	$C_{36}H_{54}N_4O_{12}Zn_3$
solvent	C_7H_8	$1.75C_4H_8O$	$2.25C_4H_8O$
fw	1075.23	1025.12	1093.18
T (°C)	−100	−100	−100
space group	$P\bar{1}$ (no. 2)	$P2_1/c$ (no. 14)	$P\bar{1}$ (no. 2)
a (Å)	10.08917(16)	24.2406(3)	20.2849(5)
b (Å)	13.7070(3)	16.3317(2)	20.4982(4)
c (Å)	19.7768(3)	29.4556(2)	23.6840(6)
α (deg)	76.4901(16)		73.361(2)
β (deg)	78.5010(13)	114.217(1)	89.007(2)
γ (deg)	80.1700(15)		61.549(2)
V (Å^3)	2583.71(8)	10635.0(2)	8212.7(4)
Z	2	8[a]	6[b]
ρ_{calcd} (g cm^{-3})	1.382	1.280	1.326
λ (Å)	0.71073[c]	0.71073[c]	1.54184[d]
μ (mm^{-1})	1.439	1.397	2.045
R_1 (obs)[e]	0.039	0.061	0.046
wR_2 (all)[f]	0.117	0.233	0.129

[a] There are two crystallographically independent molecules. [b] There are three crystallographically independent molecules. [c] Oxford Diffraction Xcalibur 3 diffractometer. [d] Oxford Diffraction Xcalibur PX Ultra diffractometer. [e] $R_1 = \sum||F_o| - |F_c||/\sum|F_o|$. [f] $wR_2 = \{\sum[w(F_o^2 - F_c^2)^2]/\sum[w(F_o^2)^2]\}^{1/2}$; $w^{-1} = \sigma^2(F_o^2) + (aP)^2 + bP$.

relatively unusual for zinc catalysts, although Xiao et al. also report no ether linkages in the polymer produced by their zinc catalyst at 1 atm of CO_2 pressure.[31] The cause of this apparent prevention of homopolymerization is still under investigation. Small quantities of cyclic carbonate (~ 4%) are always observed (Scheme 1). Other groups have also observed a cyclic carbonate byproduct whose formation has been attributed to the low ceiling temperature of copoly(cyclohexene carbonate).[13,49] The copolymer molecular weights are low; several factors contributed to this. First, as the copolymerization is carried out in neat monomer, conversions are not allowed to exceed 50%, after which a high viscosity makes stirring difficult. Second, it has been established by van Meerendonk et al., and observed in our previous report, that the polymer molecular weights are frequently much lower than expected due to side reactions between zinc catalysts and CHO, producing alcohols, which act as chain transfer agents.[42,43] Such chain transfer reactions are fast and reversible, as the polydispersity indices (Table 2, M_w/M_n) are all in the range 1.00−1.22. Third, the bimetallic complexes each have two active sites, and therefore the expected molecular weights will be one-half those of conventional monometallic catalysts, such as the salen complexes (Figure 1, **2** and **3**). When the catalyst loading is reduced to 0.01 mol %, and a higher pressure of CO_2 is used (10 atm), higher molecular weights of around 14 000 are observed.[42]

The trizinc complexes, $[L^{1-3}Zn_3(OAc)_4]$, were also tested under the same conditions (1 atm CO_2, 80 °C). The quality of the copolymers is very similar to that produced by $[L^{1-3}Zn_2(OAc)_2]$, with no detectable ether linkages and polydispersity indices of around 1.2. The molecular weights of the copolymers are even lower; however, this also corresponds to a lower percentage conversion. The polymer produced by $[L^2Zn_3(OAc)_4]$ also contained an increased amount of cyclic carbonate byproduct (11%). The three potentially active zinc sites and four acetate initiating groups might be expected to increase the catalytic activity. In order to account for this and enable direct comparisons with the bimetallic analogues, $[L^{1-3}Zn_2(OAc)_2]$, TONs and TOFs per mole of Zn were calculated for all of the catalysts (Table 2). The trimetallic catalysts showed significantly reduced activities compared to their bimetallic analogues. For example, $[L^1Zn_3(OAc)_4]$ shows a TOF slightly less than half that of $[L^1Zn_2(OAc)_2]$, an activity lower than that of $[L^3Zn_2(OAc)_2]$. The same structural trends are observed, $[L^2Zn_3(OAc)_4]$ is less active than $[L^1Zn_3(OAc)_4]$, while $[L^3Zn_3(OAc)_4]$ is significantly less active than both. The decreased activity of the trizinc complexes confirms our previous report that the macrocyclic coordination environment around the active site is vital for controlling catalyst activity.[42] A series of conclusions can be drawn: First, the zinc center external to the macrocycle is less active than the two zinc centers coordinated by the macrocycle. Second, this externally coordinated zinc center appears to hinder CO_2 and CHO binding to the catalyst. The current results indicate that the ability of the Zn−O bonds to participate in the insertion steps necessary for copolymerization are highly dependent on the electronic and steric environment around the zinc center.

Conclusions

A series of three macrocyclic proligands have been synthesized and used to prepare bimetallic and trimetallic zinc acetate complexes. All of the new complexes have been fully characterized, including by solution spectroscopic and X-ray diffraction techniques. The trimetallic complexes contain two different zinc coordination environments and several different acetate environments. All of these complexes were active catalysts for the copolymerization of CHO and CO_2, at just 1 atm of CO_2 pressure. The new catalysts all produced high-quality copolymers, without any observable ether linkages, and with low polydispersity indices. The most active of these complexes was the previously reported $[L^1Zn_2(OAc)_2]$; the introduction of a less bulky methyl group and an electron-donating methoxy group decreases the activity of the catalyst. We previously reported that monometallic and bimetallic open-ligand analogues of $[L^1Zn_2(OAc)_2]$ were inactive, stating the importance of the metal coordination environment within the macrocycle to its activity. The decreased activity of the trimetallic complexes compared to their bimetallic analogues corroborates this assertion; a zinc center external to the ligand hinders the copolymerization rather than enhancing it.

Experimental Section

Materials and Methods. The syntheses of H_2L^n and $[H_4L^{n'}](ClO_4)_2$ were carried out in the air. The syntheses of the metal complexes $[L^nZn_2(OAc)_2]$ and $[L^nZn_3(OAc)_4]$ were conducted under a nitrogen atmosphere, either using standard anaerobic techniques or in a nitrogen filled glovebox. 4-*tert*-butyl-2,6-diformylphenol, 2,6-diformyl-4-methylphenol, and 2,6-diformyl-4-methoxyphenol were synthesized according to a literature procedure.[44] All solvents and reagents were obtained from commercial sources (Aldrich and Merck). THF was

(49) Super, M.; Beckman, E. J. *Macrolmol. Symp.* **1998**, *127*, 89–108.

distilled from sodium and stored under nitrogen. Cyclohexene oxide (CHO), methylene chloride, and d_2-TCE were distilled from CaH_2 and stored under nitrogen. CP-grade carbon dioxide was used for copolymerization studies.

^1H and $^{13}C\{^1H\}$ NMR spectra were performed on a Bruker AV-400 instrument, unless otherwise stated. All mass spectrometry measurements were performed using a Fisons Analytical (VG) Autospec spectrometer. All IR spectra were performed neat on a Perkin-Elmer Spectrum 100 ATR-IR instrument. Elemental analyses were determined by Stephen Boyer at London Metropolitan University, North Campus, Holloway Road, London, N7. SEC data were collected using a Polymer Laboratories PL GPC-50 instrument with THF as the eluent, at a flow rate of 1 mL min^{-1}. Two Polymer Laboratories Mixed D columns were used in series. Narrow M_w polystyrene standards were used to calibrate the instrument.

X-Ray Crystallography. Table 3 provides a summary of the crystallographic data for compounds $[L^1Zn_3(OAc)_4]$, $[L^2Zn_3(OAc)_4]$, and $[L^3Zn_3(OAc)_4]$. CCDC numbers for the compounds are 721028−721030. For further details of the X-ray crystallography, see the Supporting Information.

General Procedure for the Synthesis of $[H_4L^{n'}](ClO_4)_2$. To a round-bottomed flask was added 4-*R*-2,6-diformylphenol (5.80 mmol), $NaClO_4$ (2.81 g, 23.2 mmol), acetic acid (0.66 mL, 11.6 mmol), and methanol (90 mL). This solution was heated to 70 °C while stirring; as the solution started to boil, 2,2-dimethyl-1,3-propanediamine (0.70 mL, 5.8 mmol) was added, slowly, in methanol (30 mL). The reaction mixture was allowed to cool to room temperature and was left stirring for 24 h, after which a precipitate was filtered and washed with cold (−78 °C) methanol.

$[H_4L^{1'}](ClO_4)_2$. Orange crystals; yield: 1.85 g, 2.76 mmol, 95%. ^1H NMR (d_6-DMSO): δ 13.61 (br s, 4H, N*H*/O*H*), 8.68 (d, 4H, N=C*H*), 7.66 (s, 4H, Ar−*H*), 3.87 (s, 8H, CH_2), 1.28 (s, 12H, CH_3), 1.15 (s, 18H, CH_3). $^{13}C\{^1H\}$ NMR (d_6-DMSO): δ 176.5, 169.3, 142.5, 136.2, 116.6, 60.7, 35.2, 34.0, 31.2, and 23.6. *m*/*z* (ES): 545.3875 (80%, $[M - H]^+$; $C_{34}H_{49}N_4O_2$ requires 545.3856).

$[H_4L^{2'}](ClO_4)_2$. Orange crystals; yield: 1.72 g, 2.26 mmol, 76%. ^1H NMR (d_6-DMSO): δ 8.63 (d, J = 13.5 Hz, 4H, N=C*H*), 7.34 (s, 4H, Ar−*H*), 3.90 (d, 8H, N−CH_2−C), 2.13 (s, 6H, Ar−CH_3), 1.28 (s, 12H, C−CH_3). $^{13}C\{^1H\}$ NMR (d_6-DMSO): δ 176.1, 168.1, 145.2, 122.5, 116.3, 60.2, 33.7, 30.4, 18.7. Anal. Calcd for $C_{28}H_{38}Cl_2N_4O_{10}$: C, 50.84; H, 5.79; N, 8.47%. Found: C, 50.79; H, 5.77; N, 8.41%.

$[H_4L^{3'}](ClO_4)_2$. Brick red powder; yield: 0.63 g, 0.90 mmol, 31%. ^1H NMR (d_6-DMSO): δ 13.83 (s, 4H, O*H*/N*H*), 8.67 (d, 4H, N=C*H*), 7.22 (s, 4H, Ar−*H*), 3.90 (s, 8H, N−CH_2−C), 3.69 (s, 6H, Ar−O−CH_3), 1.29 (s, 12H, C−CH_3). $^{13}C\{^1H\}$ NMR (d_6-DMSO): δ 174.3, 168.5, 147.3, 130.7, 116.9, 61.2, 56.4, 34.4, 23.5. Anal. Calcd for $C_{28}H_{38}Cl_2N_4O_{12}$: C, 48.49; H, 5.52; N, 8.08%. Found: C, 48.47; H, 5.46; N, 8.12%.

General Procedure for the Synthesis of $H_2L^{1,2}$ from $[H_4L^{n'}](ClO_4)_2$. $[H_4L^{n'}](ClO_4)_2$ (2.7 mmol) was suspended in methanol (180 mL). The suspension was cooled to 0 °C, and $NaBH_4$ (2.65 g, 70 mmol) was added, slowly. As $NaBH_4$ was added, the red-orange suspension turned to a clear solution. The solution was allowed to stir at room temperature for 1 h, after which water was added slowly, and the solution turned cloudy. Once the precipitate started to form, the mixture was left overnight. The product was filtered, washed with water, and dried under a vacuum to yield white crystals of the title compound.

H_2L^1. Yield: 1.21 g, 2.19 mmol, 88%. Mp 162 °C (from methanol). ^1H NMR ($CDCl_3$): δ 6.95 (s, 4H, Ar−*H*), 3.76 (s, 8H, CH_2), 2.53 (s, 8H, CH_2), 1.27 (s, 18H, CH_3), 1.02 (s, 12H, CH_3). $^{13}C\{^1H\}$ NMR ($CDCl_3$): δ 154.7, 140.7, 124.9, 124.3, 59.9, 53.4, 34.7, 34.1, 31.7, and 25.2. *m*/*z* (ES): 553 ($[M + H]^+$, 75%), 277 (100). Anal. Calcd for $C_{34}H_{56}N_4O_2$: C, 73.87; H, 10.21; N, 10.13%. Found: C, 73.87; H, 10.26; N, 10.18%.

H_2L^2. Yield: 0.75 g, 1.6 mmol, 59%. Mp 154 °C. ^1H NMR ($CDCl_3$): δ 6.74 (s, 4H, Ar−*H*), 3.74 (s, 8H, N−CH_2−Ar), 2.51 (s, 8H, N−CH_2−C), 2.22 (s, 6H, Ar−CH_3), 1.03 (s, 12H, C−CH_3). $^{13}C\{^1H\}$ NMR ($CDCl_3$): δ 154.6, 128.7, 127.2, 124.7, 59.7, 52.7, 34.7, 25.0, 20.4. *m*/*z* (ES): 469 ($[M + H]^+$, 100%), 235 (14%). Anal. Calcd for $C_{28}H_{44}N_4O_2$: C, 71.76; H, 9.46; N, 11.95%. Found: C, 71.60; H, 9.52; N, 11.88%.

Synthesis of H_2L^3 from $[H_4L^{3'}](ClO_4)_2$. $[H_4L^{3'}](ClO_4)_2$ (1.40 g, 2.02 mmol) was suspended in MeOH (110 mL). The suspension was cooled to 0 °C, and $NaBH_4$ (1.99 g, 52.6 mmol) was added, slowly. As $NaBH_4$ was added, the brick-red suspension turned to a light brown, clear solution. The solvent was removed, in vacuo, and the crude product taken up in a minimal amount of $CHCl_3$. After an hour, a brown precipitate was filtered off, and the solvent was removed in vacuo. The product was recrystallized from MeOH/H_2O and dried in vacuo. White crystals, 0.340 g, 0.68 mmol, 34%. Mp 74 °C (from $CHCl_3$). ^1H NMR ($CDCl_3$): δ 6.52 (s, 4H, Ar−*H*), 3.74 (m, 14H, N−CH_2−Ar and Ar−O−CH_3), 2.50 (s, 8H, N−CH_3−C), 1.02 (s, 12H, C−CH_3). $^{13}C\{^1H\}$ NMR ($CDCl_3$): δ 151.7, 150.5, 125.6, 113.5, 59.4, 55.7, 52.6, 34.6, 24.9. *m*/*z* (ES): 501 (100%, $[M + H]^+$), 251 (25%). Anal. Calcd for $C_{28}H_{44}N_4O_4$: C, 67.17; H, 8.86; N, 11.19%. Found: C, 67.28; H, 8.98; N, 11.06%.

Synthesis of $[L^{n}Zn_2(OAc)_2]$. H_2L^n (0.72 mmol) was dissolved in dry THF (10 mL), in a Schlenk tube. The solution was transferred to another Schlenk tube containing $Zn(OAc)_2$ (0.27 g, 1.48 mmol). The reaction was left to stir for 16 h, after which the THF was removed in vacuo and the product taken up in dry CH_2Cl_2 (10 mL). The solution was then filtered, the solvent removed in vacuo, and the white powder dried under a vacuum overnight.

$[L^1Zn_2(OAc)_2]$. Yield: 0.40 g, 0.5 mmol, 70%. ^1H NMR (d_2-TCE, 383 K): δ 7.00 (s, 4H, Ar−*H*), 4.78 (br s, 4H, N*H*), 3.32 (br d, 4H, CH_2), 2.95 (br s, 4H, CH_2), 2.84 (br s, 4H, CH_2), 2.46 (br s, ∼ 4H, CH_2), 2.08 (s, ∼ 6H, OAc), 1.35 (s, 18H, Ar−C−CH_3), 1.29 (s, 6H, CH_2−C−CH_3), 1.05 (s, 6H, CH_2−C−CH_3). $^{13}C\{^1H\}$ NMR (d_2-TCE, 383 K): δ 174.7, 159.5 (br), 139.5 (br), 127.4, 124.4, 63.2, 56.3, 33.5, 31.4, 27.9, 21.1, and 20.7. *m*/*z* (FAB): 739 ($[M - OAc]^+$, 100%). Anal. Calcd for $C_{36}H_{60}N_4O_2Zn_2$: C, 57.07; H, 7.56; N, 7.01%. Found: C, 56.91; H, 7.46; N, 6.92%.

$[L^2Zn_2(OAc)_2]$. Yield: 0.37 g, 0.52 mmol, 72%. ^1H NMR (d_2-TCE, 383 K): δ 6.83 (s, 4H, Ar−*H*), 4.76 (br s, 4H, N*H*), 3.26 (br s, 4H, CH_2), 2.96 (br s, 4H, CH_2), 2.79 (br s, 4H, CH_2), 2.44 (br s, 4H, CH_2), 2.27 (s, 6H, Ar−CH_3), 2.09 (s, 6H, OAc), 1.26 (s, 6H, C−CH_3), 1.04 (s, 6H, C−CH_3). $^{13}C\{^1H\}$ NMR (d_2-TCE, 383 K): δ 175.1, 159.0 (br), 139.0 (br), 131.0, 124.7, 63.4, 56.1, 33.4, 27.9, 21.3, 19.7. *m*/*z* (FAB): 656 ($[M - OAc]^+$, 100%). Anal. Calcd for $C_{32}H_{48}N_4O_6Zn_2$: C, 53.71; H, 6.76; N, 7.83%. Found: C, 53.60; H, 6.74; N, 7.82%.

$[L^3Zn_2(OAc)_2]$. Yield: 0.40 g, 0.54 mmol, 75%. ^1H NMR (d_2-TCE, 383 K): δ 6.61 (s, 4H, Ar−*H*), 4.68 (s, br, 4H, N*H*), 3.77 (s, 6H, Ar−OCH_3), 3.21 (s, br, 4H, CH_2), 2.98 (s, br, 4H, CH_2), 2.76 (s, br, 4H, CH_2), 2.49 (s, br, ∼4H, CH_2), 2.01 (s, 6H, OAc), 1.25 (s, 6H, C−CH_3), 1.03 (s, 6H, C−CH_3). $^{13}C\{^1H\}$ NMR (d_2-TCE, 383 K): δ 174.5, 155.2, 150.4, 125.5, 116.2, 63.2, 56.8, 33.4, 27.8, 21.4, 20.8. *m*/*z* (FAB): 687 ($[M - OAc]^+$, 98%). Anal. Calcd for $C_{32}H_{48}N_4O_8Zn_2$: C, 51.42; H, 6.47; N, 7.49%. Found: C, 51.36; H, 6.56; N, 7.49%.

Synthesis of $[L^{n}Zn_3(OAc)_4]$. H_2L^n (0.72 mmol) was dissolved in dry THF (10 mL), in a Schlenk tube. The solution was transferred to a Schlenk tube containing $Zn(OAc)_2$ (0.54 g, 2.96 mmol). The reaction was left to stir for 16 h, after which the THF was removed in vacuo and the product taken up in dry CH_2Cl_2 (10 mL). The solution was then filtered to remove excess $Zn(OAc)_2$ and the solvent removed in vacuo. The product was then recrystallized from THF/hexane, filtered, and washed with hexane. All NMR resonances are reported for the major isomer.

$[L^1Zn_3(OAc)_4]$. Yield: 0.57 g, 0.57 mmol, 80%. IR ($\nu_{C=O}$, cm^{-1}, neat): 1670 and 1369 (terminal OAc), 1589 and 1426

(bridging OAc). ^{1}H NMR (CD_3OD): δ 7.09 (s, 4H, Ar−*H*), 4.28 (t, 4H, N*H*), 3.26 (d, 4H, C*H*$_2$), 3.03 (t, 4H, C*H*$_2$), 2.77 (m, 8H, C*H*$_2$), 1.80 (s, 12H, OAc), 1.29 (s, br, 18H, Ar−C−C*H*$_3$), 1.27 (d, 6H, N−C−C*H*$_3$), 1.03 (s, 6H, N−C−C*H*$_3$). ^{13}C{^{1}H} NMR (d_2-TCE, 383 K): δ 177.2, 159.8 (br), 139.8 (br), 127.9, 125.0, 62.1, 55.2, 33.7, 33.3, 31.4, 28.2, 22.6, 20.8. *m*/*z* (FAB): 740 ([M − Zn(OAc)$_3$]$^+$, 100%). Anal. Calcd for $C_{42}H_{66}N_4O_{10}Zn_3$: C, 51.31; H, 6.77; N, 5.70%. Found: C, 51.42; H, 6.81; N, 5.64%.

[L^{2}Zn$_3$(OAc)$_4$]. Yield: 0.53 g, 0.59 mmol, 82%. IR ($\nu_{C=O}$, cm^{-1}, neat): 1705 and 1381 (terminal OAc), 1583 and 1423 bridging OAc). ^{1}H NMR (CD_3OD): δ 6.87 (s, 4H, Ar−*H*), 4.22 (m, 4H, N*H*), 3.21 (d, 4H, C*H*$_2$), 2.99 (d, br, 4H, C*H*$_2$), 2.75 (m, 8H, C*H*$_2$), 2.19 (s, 6H, Ar−C*H*$_3$), 1.88 (s, br, 12H, OAc), 1.26 (s, 6H, N−C−C*H*$_3$), 1.02 (s, 6H, N−C−C*H*$_3$). ^{13}C{^{1}H} NMR (d_2-TCE, 383 K): δ 177.1, 160.0 (br), 144.2 (br), 131.8, 125.5, 62.2, 54.8, 33.8, 28.2, 22.5, 20.7, 19.7. *m*/*z* (FAB): 656 ([M − Zn(OAc)$_3$]$^+$, 100%). Anal. Calcd for $C_{36}H_{54}N_4O_{10}Zn_3$: C, 48.09; H, 6.05; N, 6.23%. Found: C, 48.01; H, 5.98; N, 6.11%.

[L^{3}Zn$_3$(OAc)$_4$]. Yield: 0.51 g, 0.55 mmol, 76%. IR ($\nu_{C=O}$, cm^{-1}, neat): 1651 and 1379 (terminal OAc), 1587 and 1427 (bridging OAc). ^{1}H NMR (CD_3OD): δ 6.65 (s, 4H, Ar−*H*) 4.22 (d, 4H, C*H*$_2$), 3.70 (s, 6H, OC*H*$_3$), 3.17 (d, 4H, C*H*$_2$), 2.97 (d, 4H, C*H*$_2$), 2.65 (d, 4H, C*H*$_2$), 1.80 (s, br, 12H, OAc), 1.24 (s, 6H, C*H*$_3$), 1.00 (s, 6H, C*H*$_3$). ^{13}C{^{1}H} NMR (CD_3OD): 180.1, 157.6 (br), 152.2 (br), 127.4, 118.0, 63.4, 56.2, 55.8, 34.9, 28.7, 23.0, 21.2. *m*/*z* (FAB): 688 ([M − Zn(OAc)$_3$]$^+$, 100%). Anal. Calcd for $C_{36}H_{54}N_4O_{12}Zn_3$: C, 46.44; H, 5.85; N, 6.02%. Found: C, 46.52; H, 5.90; N, 5.91%.

Copolymerization Conditions. Cyclohexene oxide (5 mL, 49.4 mmol) and [L^{n}Zn$_x$(OAc)$_y$] (0.049 mmol) were added to a Schlenk tube. The cyclohexene oxide was degassed, before being left to stir under 1 atm of CO_2, at 80 °C, for 24 h. The crude reaction mixture was then taken up in CH_2Cl_2 and evaporated in the air, after which the product was dried in vacuo overnight. No further purification of the polymer was undertaken, as the vacuum was sufficient to remove unreacted cyclohexene oxide.

The turnover number was calculated as [(isolated yield − weight catalyst)/142.1]/moles of zinc.

The copolymers were analyzed by ^{1}H NMR spectroscopy, where the protons adjacent to the carbonate linkage resonated at 4.6 ppm, while the absence of a peak at 3.45 ppm showed that there were no polyether linkages. The copolymer tacticity was determined by ^{13}C{^{1}H} NMR spectroscopy and analyzed as described by Nozaki et al.[50] The copolymers were all atactic.

Acknowledgment. The EPSRC is acknowledged for funding this research (EP/C544846/1 and EP/C544838/1).

Supporting Information Available: Additional figures and a CIF file. This material is available free of charge via the Internet at http://pubs.acs.org.

(50) Nozaki, K.; Nakano, K.; Hiyama, T. *J. Am. Chem. Soc.* **1999**, *121*, 11008–11009.